

AN INSTRUMENTAL VARIABLE METHOD FOR ROBOT IDENTIFICATION BASED ON TIME VARIABLE PARAMETER ESTIMATION

MATHIEU BRUNOT, ALEXANDRE JANOT, PETER C. YOUNG
AND FRANCISCO CARRILLO

This paper considers the data-based identification of industrial robots using an instrumental variable method that uses off-line estimation of the joint velocities and acceleration signals based only on the measurement of the joint positions. The usual approach to this problem relies on a ‘tailor-made’ prefiltering procedure for estimating the derivatives that depends on good prior knowledge of the system’s bandwidth. The paper describes an alternative Integrated Random Walk SMOOTHING (IRWSM) method that is more robust to deficiencies in such a priori knowledge and exploits an optimal recursive algorithm based on a simple integrated random walk model and a Kalman filter with associated fixed interval smoothing. The resultant IDIM-IV instrumental variable method, using this approach to signal generation, is evaluated by its application to an industrial robot arm and comparison with previously proposed methods.

Keywords: industrial robot system, system identification, instrumental variable method, parameter estimation, Kalman filter, fixed interval smoothing

Classification: 93B30 , 70E60

1. INTRODUCTION

For many years, the most common method used for robot identification has been based on Least-Squares (LS) optimization and estimation of the Inverse Dynamic Identification Model (IDIM): see e. g. [9] or [10]. The IDIM expresses the input torque as a linear function of the physical parameters thanks to the modified Denavit and Hartenberg (DHM) notation: see e. g. [15]. Although this is a popular and quite successful method, it is not always robust to the measurement noise correlation that arises from the closed-loop structure required for robot operation.

In order to avoid possible bias in the model parameter estimates, an Instrumental Variable (IV) method has been suggested and successfully evaluated on robot systems [14]. Like the IDIM-LS method, however, this IDIM-IV approach requires well-tuned, bandpass filtering to generate the velocity and acceleration signals from the joint position measurements. Consequently, the requirement for good a priori knowledge of the system bandwidth may well be an issue during early tests of the system, especially

if there is no access to the key design parameters, as when a robot is purchased ‘off-the-shelf’.

The aim of this paper is, therefore, to extend the IDIM-IV method by estimating the joint derivatives in an automated way, with the model structure assumed known, since it is based on the laws of mechanics, but without a priori knowledge of the associated parameters values. This research is related to that presented in [2], where the derivatives were estimated and used only for use with the IDIM-LS method. As in this previous study, the identification procedure is evaluated and validated on a 6 degrees of freedom industrial robot.

The issue of differentiating numerical signals has been raised in many scientific fields. In the system identification community, it has been successfully tackled by different techniques such as the generalized Poisson moment functional (GPMF) in [19], which follows directly to the earlier Method of Multiple Filters (MMF) and the more general State Variable Filters (SVF) in [16, 23], or the Refined Instrumental Variable (RIVC) in [7, 27], for instance. For further reading on the topic, see e.g. [8, 24]. However, these methods are designed mainly for linear systems and so they are not relevant for the present study, although they do provide some clues about how to handle differentiation in the case on nonlinear systems. Instead, we consider an off-line prefiltering technique based on a simple but flexible ‘generalised random walk’ model for the signal variations, with the time derivative estimates generated by a Kalman filter and associated Fixed Interval Smoother (FIS). This was first suggested in [26] for linear systems and then used in [4] for nonlinear systems.

This paper is organised as follows. Section 2 outlines the main aspects of the IDIM-IV method for robot identification. The off-line method of multiple differentiation of sampled signals, based on a Kalman filter and FIS, is investigated from a robot identification perspective in section 3. Then this approach is evaluated using experimental data from a Stäubli TX40 industrial robot arm, by considering three cases. First, we assume good a priori knowledge on the system, which allows for ‘tailor-made’ bandpass filtering; second, inadequate bandpass filtering is assumed, due to a lack of knowledge about the robot characteristics; finally, an ultimate test, without any prior knowledge, is undertaken. The conclusions are presented in section 5.

2. ROBOT IDENTIFICATION

2.1. Robot dynamic models

For a robot with n moving links, the $(n \times 1)$ vector $\boldsymbol{\tau}_{dm}(t)$ regroups the input torques or forces of those links. The joint positions, velocities and accelerations are contained in the $(n \times 1)$ vectors $\boldsymbol{q}(t)$, $\dot{\boldsymbol{q}}(t)$ and $\ddot{\boldsymbol{q}}(t)$ respectively. The following vector equation is then derived by application of Newton’s second law:

$$\boldsymbol{M}(\boldsymbol{q}(t))\ddot{\boldsymbol{q}}(t) = \boldsymbol{\tau}_{dm}(t) - \boldsymbol{N}(\boldsymbol{q}(t), \dot{\boldsymbol{q}}(t)) \quad (1)$$

where, $\boldsymbol{M}(\boldsymbol{q}(t))$ is the $(n \times n)$ inertia matrix of the robot, and $\boldsymbol{N}(\boldsymbol{q}(t), \dot{\boldsymbol{q}}(t))$ is the $(n \times 1)$ vector representing the disturbances or perturbations. The friction forces, gravity effects and other non-linearities, depending on the specific robot being considered, are included in these perturbations. From experience, we know that, in the vast majority of cases, the

disturbances are linear in the parameters but not in the states: see e. g. [15]. Therefore, the input torques appear to be linear with respect to the parameters. The Inverse Dynamic Model (IDM) exploits this and is defined as the following equation, where the input torques are a function of the outputs:

$$\boldsymbol{\tau}_{idm}(t) = \boldsymbol{\phi}(\mathbf{q}(t), \dot{\mathbf{q}}(t), \ddot{\mathbf{q}}(t)) \boldsymbol{\theta}. \quad (2)$$

Here, the input torques can be interpreted as the dependent (or observation) variables; $\boldsymbol{\phi}$ is the $(n \times b)$ observation matrix composed of regressors (or independent variables); $\boldsymbol{\theta}$ is the $(b \times 1)$ vector of base parameters that need to be estimated. Finally, as a result of perturbations coming from measurement noise and modelling errors, the actual torques $\boldsymbol{\tau}(t)$ differ from $\boldsymbol{\tau}_{idm}(t)$ by an error term $\mathbf{v}(t)$. The full stochastic IDIM is then given by:

$$\boldsymbol{\tau}(t) = \boldsymbol{\tau}_{idm}(t) + \mathbf{v}(t) = \boldsymbol{\phi}(\mathbf{q}(t), \dot{\mathbf{q}}(t), \ddot{\mathbf{q}}(t)) \boldsymbol{\theta} + \mathbf{v}(t). \quad (3)$$

The Direct Dynamic Model (DDM) is the following alternative form of the model equations that expresses the joint accelerations as a function of the torques, as well as the joint positions and velocities:

$$\ddot{\mathbf{q}}(t) = \mathbf{M}(\mathbf{q}(t))^{-1} (\boldsymbol{\tau}_{idm}(t) - \mathbf{N}(\mathbf{q}(t), \dot{\mathbf{q}}(t))). \quad (4)$$

The DDM is not used directly for the identification because the joint accelerations are nonlinear with respect to the parameters and so they are more difficult to estimate. However, this DDM is more convenient for simulation purposes and is used as such in section 2.2.

2.2. The IDIM-IV method

The Instrumental Variable (IV) approach to model parameter estimation also exploits the IDIM model form but the least squares estimation is replaced by IV estimation. In this case, an $(n \times b)$ instrumental matrix, denoted by $\boldsymbol{\zeta}$, is introduced that must fulfil the following conditions:

- $\boldsymbol{\zeta}^T \boldsymbol{\phi}_{F_p}$ is full column rank,
- $\mathbb{E}[\boldsymbol{\zeta}^T \mathbf{v}_{F_p}] = 0$,

where $\boldsymbol{\phi}_{F_p}$ and \mathbf{v}_{F_p} are, respectively, the observation matrix and the error vector, in which each element is filtered by the decimation filter, F_p ; while $\mathbb{E}[\cdot]$ denotes the mathematical expectation. The first condition means that the instrumental matrix must be well correlated with the observations and is sometimes termed the *instrument relevance* [22]. The second condition expresses the fact that the instrumental matrix must be uncorrelated with the error and is sometimes known as the *instrument exogeneity*. Assuming that the two previous conditions hold, it can be shown that the IV parameter estimates $\hat{\boldsymbol{\theta}}_{IV}(N)$ given by

$$\hat{\boldsymbol{\theta}}_{IV}(N) = \left[\frac{1}{N} \sum_{i=1}^N \boldsymbol{\zeta}^T(t_i) \boldsymbol{\phi}_{F_p}(t_i) \right]^{-1} \left[\frac{1}{N} \sum_{i=1}^N \boldsymbol{\zeta}^T(t_i) \boldsymbol{\tau}_{F_p}(t_i) \right], \quad (5)$$

are asymptotically unbiased and consistent. In this IV solution, N is the number of sampling points considered for the identification and $\tau_{F_p}(t_i) = F_p(z^{-1})\tau(t_i)$, where z^{-1} is the backward shift operator. Note that the standard LS solution is obtained if ζ is replaced by ϕ_{F_p} but that, in general when there is noise on the data, the resulting estimates will be asymptotically biased and inconsistent.

During the last decade, different IV solutions have been developed for closed-loop identification; see e.g. [12]. One key feature of the IV method is the construction of the instruments; i.e. the elements of the instrumental matrix. There are a number of ways in which they can be constructed, see e.g. [20], but it has been found that by far the most successful of these is to generate the instruments using an *auxiliary model* of the system: see e.g. [24] and the prior references therein. In [13], it has been shown that the simulation of the whole robotic system using the DDM, including the inherent closed-loop, provides a very convenient auxiliary model. The simulation of this auxiliary model provides noise-free simulated signals that are used to construct the instrumental matrix using the same equations as those of the observation matrix. If the parameters of this auxiliary model are reasonable and there is no modelling error, the IV requirements will be satisfied and the resulting estimates will have the required properties. This is because the simulated signals are noise-free, since the only input to the simulation is the reference trajectory and this is known perfectly.

In order to ensure the efficacy of the parameters in the auxiliary model, the IDIM-IV method, like many IV-based methods of estimation, is an iterative process in which the estimates of the parameters from the previous iteration are used for the auxiliary model on the next iteration. In the case of linear systems, it has been shown [25] that, in an optimal situation, this kind of iterative procedure converges to a local minimum of the cost function-parameter hyperspace. This cannot be guaranteed in this nonlinear situation but experience with the IDIM-IV algorithm shows that it is robust in this sense; see e.g. [3, 13].

By noting the simulated signals with a subscript s , the instrumental matrix at iteration it is:

$$\zeta(t, \hat{\theta}_{IV}^{it}) = F_p(z^{-1})\phi \left(\mathbf{q}_s(t, \hat{\theta}_{IV}^{it}), \dot{\mathbf{q}}_s(t, \hat{\theta}_{IV}^{it}), \ddot{\mathbf{q}}_s(t, \hat{\theta}_{IV}^{it}) \right) \quad (6)$$

and the complete iterative process can be described as follows:

1. **Initialisation.** For the initial physical parameters, $\hat{\theta}^0$, we use the Computed-Aided Design (CAD) values for the inertia. The other physical parameters are set to zero. The observation matrix must be constructed in relation to the IRWSM technique proposed here for differentiating the position signals, as discussed in the next section 3, which ensures a systematic and optimal differentiation process.
2. **Iteration:** repeat the following steps until convergence (it stands for the it th iteration)
 - (a) Simulate the auxiliary model (i.e. the DDM) to retrieve the noise-free signals for the instruments by using $\hat{\theta}^{it-1}$.
 - (b) Compute the latest IV estimate of the physical parameters using

$$\hat{\theta}^{it} = \left[\frac{1}{N} \sum_{i=1}^N \zeta^T(t_i, \hat{\theta}^{it-1}) \phi_{F_p}(t_i) \right]^{-1} \left[\frac{1}{N} \sum_{i=1}^N \zeta^T(t_i, \hat{\theta}^{it-1}) \tau_{F_p}(t_i) \right]. \quad (7)$$

3. **Estimated covariance.** After convergence, the estimated parametric error covariance matrix of the physical parameters is computed from the following relation

$$P(\hat{\theta}) = \left\{ \frac{1}{N} \sum_{i=1}^N \zeta^T(t_i, \hat{\theta}) \hat{\Lambda}^{-1} \zeta(t_i, \hat{\theta}) \right\}^{-1}, \quad (8)$$

where $\hat{\Lambda}$ is the $(n \times n)$ estimated covariance matrix of the filtered error \mathbf{v}_{F_p} and $\hat{\theta}$ is the vector of estimated parameters.

It should be noticed that (8) is an approximation to the real covariance formula. The underlying assumption is that the instrumental matrix has converged to the noise-free part of the observation matrix and that the residual error is a zero mean, serially uncorrelated sequence of random variables with a normal distribution ('white noise'). The convergence criterion is composed of two complementary tests: one on the relative variation of the estimated torques and one on the relative variation of the estimated parameters: see e.g. [13] for further details.

3. SIGNAL PREFILTERING AND DIFFERENTIATION

The prefiltering of the position signals to generate the velocity and acceleration signals required for IDIM-IV parameter estimation is an essential part of the robot identification procedure proposed in the present paper. The conventional approach (see e.g. [10]) relies on the user's skills and knowledge of the robot characteristics: it involves four steps that include bandpass filtering at a user specified frequency, applied forward and backward to avoid phase lag, as well as final re-sampling at a lower frequency (down-sampling). This section considers an alternative method of off-line signal processing that generates lag-free estimates of the velocity and acceleration signals. This approach exploits a combination of the Kalman Filter and recursive Fixed Interval Smoothing (KF/FIS) algorithms and it derives originally from the systems and control literature: see [18] and section 4.5 of chapter 4 in [24], which provides a full description of the general approach applied to a variety of different state-space model forms. The associated state-space model is a particularly simple Generalised Random Walk (GRW) process and the resulting Integrated Random Walk SMoothing (IRWSM) algorithm is outlined below both for reference and the convenience of the reader. This algorithm is available as the `irwsm` routine in the CAPTAIN Toolbox¹ for Matlab[®].

3.1. The state space model: IRW

There are a number of publications on the numerical differentiation issue (see e.g. [5] and the cited references therein). The advantage of the IRWSM algorithm in this regard

¹This Toolbox is available free and can be downloaded via <http://captaintoolbox.co.uk>.

is that it does not depend on a priori knowledge of the system and involves a quite simple, user-friendly computational process, without requiring a detailed dynamic model of the kind required, for instance, by the various procedures discussed in [5].

Equation (9) below defines the GRW state vector in the simplest case that is relevant in the present context, with $x(k)$ the joint position state at the k th sampling instant; and $\nabla x(k)$ its rate of change, the velocity of the joint at this same sampling instant. However, we will see later how this is easily extended to include other elements if higher order time derivatives, such as the acceleration, are required. Equation (10) is the associated state equation for the GRW process; and equation (11) is the observation equation.

$$\mathbf{x}(k) = \begin{bmatrix} x(k) \\ \nabla x(k) \end{bmatrix} \quad (9)$$

$$\mathbf{x}(k) = \mathbf{A}\mathbf{x}(k-1) + \mathbf{D}\boldsymbol{\eta}(k-1) \quad (10)$$

$$y(k) = \mathbf{h}(k)\mathbf{x}(k) + e(k). \quad (11)$$

In these equations,

$$\mathbf{A} = \begin{bmatrix} \alpha & \beta \\ 0 & \gamma \end{bmatrix}, \quad \mathbf{D} = \begin{bmatrix} \delta & 0 \\ 0 & \kappa \end{bmatrix} \quad (12)$$

and \mathbf{h} is a suitably defined row vector. $\boldsymbol{\eta}(k)$ is the state noise, assumed to be a white noise vector with zero mean value and associated, normally assumed diagonal, covariance matrix \mathbf{Q}_η with elements $\mathbf{Q}_{\eta_{11}}$ and $\mathbf{Q}_{\eta_{22}}$. The measurement noise $e(k)$ is also assumed to be zero mean and white, with covariance σ_e^2 . Many variants of this GRW model exist [24], depending on the choice of the hyper-parameters $[\alpha \ \beta \ \gamma \ \delta \ \kappa \ \mathbf{Q}_{\eta_{11}} \ \mathbf{Q}_{\eta_{22}}]$. For this study, the *Integrated Random Walk* (IRW: $\alpha = \beta = \gamma = \kappa = 1$, $\delta = 0$ and $\mathbf{h} = [1 \ 0]$) is considered first. In this case, $\delta = 0$, so that the term $\mathbf{Q}_{\eta_{11}}$ has no influence and is set equal to $\mathbf{Q}_{\eta_{22}}$ in order to preserve the definite-positive property of the covariance matrix. As we shall see below, a suitably normalised value of $\mathbf{Q}_{nvr} = \mathbf{Q}_{\eta_{22}}/\sigma_e^2$, the Noise Variance Ratio (NVR), can be estimated using Maximum Likelihood (ML) optimisation or chosen by the user.

3.2. The Kalman and FIS equations

The IRWSM algorithm described fully in [24] is summarized below.

Prediction step:

$$\hat{\mathbf{x}}(k|k-1) = \mathbf{A}\hat{\mathbf{x}}(k-1) \quad (13)$$

$$\mathbf{P}(k|k-1) = \mathbf{A}\mathbf{P}(k-1)\mathbf{A}^T + \mathbf{D}\mathbf{Q}_{nvr}\mathbf{D}^T. \quad (14)$$

Correction step:

$$\hat{\mathbf{x}}(k|k) = \hat{\mathbf{x}}(k|k-1) + \mathbf{g}(k)[y(k) - \mathbf{h}(k)\hat{\mathbf{x}}(k|k-1)] \quad (15)$$

$$\mathbf{g}(k) = \mathbf{P}(k|k-1)\mathbf{h}(k)[1 + \mathbf{h}(k)\mathbf{P}(k|k-1)\mathbf{h}^T(k)]^{-1} \quad (16)$$

$$\mathbf{P}(k|k) = \mathbf{P}(k|k-1) - \mathbf{g}(k)\mathbf{h}(k)\mathbf{P}(k|k-1) \quad (17)$$

$$\mathbf{P}^*(k|k) = \hat{\sigma}_e^2\mathbf{P}(k|k). \quad (18)$$

Smoothing step:

$$\widehat{\mathbf{x}}(k|N_s) = \mathbf{A}^{-1} [\widehat{\mathbf{x}}(k+1|N_s) + \mathbf{D}\mathbf{Q}_\eta\mathbf{D}^T\boldsymbol{\lambda}(k)] \quad (19)$$

$$\boldsymbol{\lambda}(k-1) = \left[\mathbf{I} - \mathbf{P}^*(k|k) \frac{\mathbf{h}^T(k)\mathbf{h}(k)}{\widehat{\sigma}_e^2} \right]^T \left(\mathbf{A}^T\boldsymbol{\lambda}(k) - \frac{\mathbf{h}^T(k)}{\widehat{\sigma}_e^2} [y(k) - \mathbf{h}(k)\mathbf{A}\widehat{\mathbf{x}}(k-1|k-1)] \right) \quad (20)$$

with $\boldsymbol{\lambda}(N_s) = 0$

$$\mathbf{P}^*(k|N_s) = \mathbf{P}^*(k|k) + \mathbf{P}^*(k)\mathbf{A}^T\mathbf{P}^*(k+1|k)^{-1} \left[\mathbf{P}^*(k+1|N_s) - \mathbf{P}^*(k+1|k) \right] \mathbf{P}^*(k+1|k)^{-1}\mathbf{A}\mathbf{P}^*(k|k). \quad (21)$$

Finally, the observation noise covariance, σ_e^2 , is estimated at the end of the filtering process in order to obtain the state covariance matrix, \mathbf{P}^* , for the smoothing process, i. e.,

$$\begin{aligned} \widehat{\sigma}_e^2 &= \frac{1}{N_s - n_x} \sum_{k=n_x+1}^{N_s} \frac{(y(k) - \mathbf{h}(k)\widehat{\mathbf{x}}(k|k-1))^2}{1 + \mathbf{h}(k)\mathbf{P}(k|k-1)\mathbf{h}^T(k)}, \\ &= \frac{1}{N_s - n_x} \sum_{k=n_x+1}^{N_s} \frac{\varepsilon^2(k)}{\nu(k)}. \end{aligned} \quad (22)$$

Here n_x is the size of the state vector ($n_x = 2$ for the IRW) and N_s is the number of sampling points. In the time domain, the first order derivative of the signal is then approximated as follows $\frac{dx}{dt}(t_k) \approx \frac{\widehat{\nabla}x(k)}{t_{k+1}-t_k}$, with $\widehat{\nabla}x(k)$ the second term of the estimated state vector $\widehat{\mathbf{x}}(k|N_s)$. Note that the sampling interval $T_s = t_{k+1} - t_k$ can be specified in the `irwsm` routine and so this is handled automatically. Also it is straightforward to augment $\mathbf{x}(k)$ with $\nabla^2x(k)$ in order to estimate the acceleration and this is a straightforward option in the `irwsm` routine.

3.3. Hyper-parameter optimisation

One advantage of the IRWSM algorithm, in relation to the standard Kalman filter, is that the user does not have to provide both the system and observation noise covariance information because these are subsumed in the NVR, which is the only hyper-parameter that needs to be specified by the user. Moreover, the CAPTAIN Toolbox provides a routine `irwsmopt` that estimates this hyper-parameter by maximizing likelihood based on minimization of the squared prediction error, $\varepsilon^2(k)$, defined in (22) (see e. g. [6]). Although this simplifies the user's task considerably, it is still necessary, of course, to assess the results in order to ensure that these are satisfactory.

3.4. Application to robot identification

The idea for robot identification is to replace the conventional prefiltering and differentiation by the IRWSM technique. The generic state space model defined by (10) and (11) needs, therefore, to be reconsidered from a robotic perspective.

Observation equation

Here, the output $y(k)$ is replaced by the measured position of link j : q_{m_j} . By considering the link j , we have the following relation for the measured position:

$$q_{m_j}(k) = q_j(k) + \tilde{q}_j(k), \quad (23)$$

where $q_j(k)$ is the joint position measured at the k th sampling instant and $\tilde{q}_j(k)$ is the sensor noise. According to [1], this noise can be considered to be white with a covariance $\frac{1}{3}\Delta_q^2$, where Δ_q is the encoder resolution; and according to [17], the Stäubli® TX40 encoders' resolution is $2 \cdot 10^{-4}$ degrees per count. This is the robot considered later for the experimental validation, which is a typical example of an industrial robot. If the measurement noise is also assumed to be normally distributed, the observation relation (11) is valid and the noise standard deviation $\sigma_e \approx \Delta_q$ can be estimated from the robot performance data sheet should it be required. Furthermore, the position $q_j(k)$ is equal to the state $x(k)$ defined by (9).

State equation

There are two ways of retrieving the joint acceleration when using IRWSM:

- Applying the algorithm twice with $\mathbf{A}_{irwsm1} = \begin{bmatrix} 1 & 1 \\ 0 & 1 \end{bmatrix}$;
- Applying the algorithm once with an augmented matrix $\mathbf{A}_{irwsm2} = \begin{bmatrix} 1 & 1 & 0 \\ 0 & 1 & 1 \\ 0 & 0 & 1 \end{bmatrix}$.

In the first case, the relevance of the random walk model is firstly investigated with \mathbf{A}_{irwsm1} . From equation (10),

$$IRWSM_1 : \begin{bmatrix} q_j(k) \\ \nabla q_j(k) \end{bmatrix} = \begin{bmatrix} 1 & 1 \\ 0 & 1 \end{bmatrix} \begin{bmatrix} q_j(k-1) \\ \nabla q_j(k-1) \end{bmatrix} + \begin{bmatrix} 1 & 0 \\ 0 & 1 \end{bmatrix} \begin{bmatrix} 0 \\ \eta_{1,j}(k-1) \end{bmatrix} \quad (24)$$

where the second state ∇q_j represents the velocity, so that velocity information is not driven by dynamic equations but by a random walk with a white noise input $\eta_{1,j}$ representing the unmodelled dynamics, effectively the modelling error. As explained in [24], this kind of model works for systems with slowly varying states. For robotic applications, however, the controller requires high frequency sampling in order to have the large feedback gains required for more robust control; see e.g. [15]. For example, the robot considered in the next section 4 has a sampling rate of 5000 Hz. However, the mechanical bandwidth is usually located below 10 Hz so, with the above IRW model expressed at the robot sampling frequency, the assumption of a slowly varying state is satisfied.

In the second case, using the augmented model transition matrix \mathbf{A}_{irwsm2} , the velocity is driven by the acceleration, which is now defined as a random walk driven by a white noise input; and, as in the case of the velocity, the assumption of a slowly varying state

seems appropriate. From (10), the state equations in this case are as follows:

$$IRWSM_2 : \begin{bmatrix} q_j(k) \\ \nabla q_j(k) \\ \nabla^2 q_j(k) \end{bmatrix} = \begin{bmatrix} 1 & 1 & 0 \\ 0 & 1 & 1 \\ 0 & 0 & 1 \end{bmatrix} \begin{bmatrix} q_j(k-1) \\ \nabla q_j(k-1) \\ \nabla^2 q_j(k-1) \end{bmatrix} + \begin{bmatrix} 1 & 0 & 0 \\ 0 & 1 & 0 \\ 0 & 0 & 1 \end{bmatrix} \begin{bmatrix} 0 \\ 0 \\ \eta_{2,j}(k-1) \end{bmatrix}. \quad (25)$$

Numerical approximation

The modelling error information can be retrieved from the tracking error, i. e.,

$$\epsilon_{tr_j}(k) = q_{r_j}(k) - q_{m_j}(k) \quad \forall k = 1, 2, \dots, N_s, \quad (26)$$

where $q_{r_j}(k)$ is the reference trajectory of link j at the k th sampling instant. Of course if the model was perfect, the tracking error would be zero $\forall k$. If the tracking error variation $\Delta\epsilon_{tr_j}(k) = \epsilon_{tr_j}(k) - \epsilon_{tr_j}(k-1)$ is assumed to be a white and normally distributed noise, we have $\eta_{1,j}(k) \approx \Delta\epsilon_{tr_j}(k)$. If the 2nd variation $\Delta^2\epsilon_{tr_j}$ is then assumed to be white and normally distributed noise, we have $\eta_{2,j}(k) \approx \Delta^2\epsilon_{tr_j}(k)$. Finally, the NVR of link j can be approximated by

$$\widehat{\text{NVR}}_j^{irwsm1} = \left(\frac{\text{std}(\Delta\epsilon_{tr_j})}{\Delta_{q_j}} \right)^2 \quad (27)$$

$$\widehat{\text{NVR}}_j^{irwsm2} = \left(\frac{\text{std}(\Delta^2\epsilon_{tr_j})}{\Delta_{q_j}} \right)^2 \quad (28)$$

where Δ_{q_j} is the encoder resolution of link j and $\text{std}(\cdot)$ is the standard deviation. Table 1 provides the estimation of the NVR considering both models. where the hyper-

Link	1	2	3	4	5	6
Δ_{q_j} (10^{-3} deg)	0.057	0.057	0.122	0.114	0.122	0.172
$\widehat{\text{NVR}}_j^{irwsm1}$	0.1476	0.1567	0.5846	0.2940	1.1101	0.6645
$\widehat{\text{NVR}}_j^{irwsm2}$	0.1951	0.2222	0.1521	0.2162	0.7491	1.6106
$\widehat{\text{NVR}}_j^{irwsm1}$	2.5368	2.2643	3.6919	2.5581	4.9713	3.8572
$\widehat{\text{NVR}}_j^{irwsm2}$	0.0015	0.0019	0.0037	0.0104	0.0045	0.0165

Tab. 1. Estimated NVR.

parameters $\widehat{\text{NVR}}_j^{irwsm1}$ and $\widehat{\text{NVR}}_j^{irwsm2}$ are estimated with the `irwsmpopt` function; and the experimental data used here are the same as those used below in section 4. The encoders' resolutions come from the data-sheet [21]. Regarding the $IRWSM_1$ option, if there is not a perfect matching between the estimated values, the orders of magnitude are the same; except for link 6. However, for the $IRWSM_2$ option, the estimated values are not comparable. This finding suggests that $\Delta^2\epsilon_{tr_j}$ cannot be seen as a white normally distributed noise and this confirmed by Figure 1 which gives the histograms

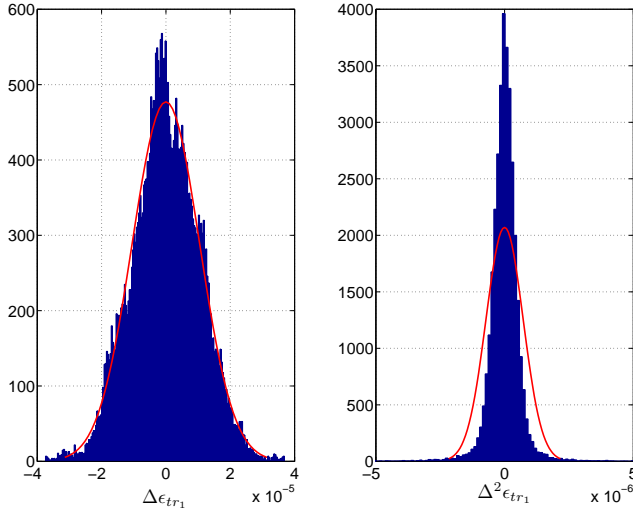


Fig. 1. Histograms with normal distribution fits – Link 1.

of $\Delta\epsilon_{tr_1}$ and $\Delta^2\epsilon_{tr_1}$ as well as normal distribution fits. For sake of clarity, only link 1 is presented here.

It is not intended that this practical reasoning should replace the `irwsmoft` function; it is simply to illustrate the relevance of the IRWSM technique for our application, where the goal is to provide an automatic solution to the practitioner. To summarize, the IRW model seems a valid solution for the estimation of the joint time derivatives, assuming the modelling error is white and normally distributed. And in this regard, the IRWSM1 option appears to be more appropriate. The following section 4 describes experimental validation of this approach using IDIM-IV estimation of the Stäubli[®] TX40 robot model parameters.

4. EXPERIMENTAL RESULTS

4.1. Robot Description

The industrial Stäubli[®] TX40 robot shown in Figure 2 is a serial manipulator composed of six rotational joints. There is a coupling between the joints 5 and 6 that adds two parameters: fv_{m6} and fc_{m6} , which are, respectively, the viscous and Coulomb friction coefficients of the motor 6. The symbolic expressions of the IDM were automatically calculated with the SYMORO + software [15]. This robot has 60 base dynamic parameters. From those base parameters, only 28 are identified with good relative standard deviations. This set of 28 parameters defines the essential parameters that are sufficient to describe the robot dynamics and it is the estimation of these parameters that we consider here (this set was validated with a F-statistic, as shown in [14]).



Fig. 2. TX40 Staubli robot.

The reference trajectories are trapezoidal velocities (also called smoothed bang-bang accelerations). Since $\text{cond}(\phi_{F_p}) = 200$, the reference trajectories provide sufficient excitation for parameter estimation, in accordance with the methodology developed in [11]. The joint positions and control signals are stored with a measurement frequency of $f_m = 5$ kHz. For the IDIM-LS method, using the conventional differentiation approach, the filter cut-off frequencies are tuned according to [10]: $\omega_{f_q} = 5\omega_{dyn} = 50$ Hz and $\omega_{F_p} = 2\omega_{dyn} = 20$ Hz, respectively, for the Butterworth and the decimation filters. The maximum bandwidth for joint 6 is $\omega_{dyn} = 10$ Hz.

Four model identification methods are compared. The first is the usual IDIM-LS approach, with the conventional approach to differentiation; the second is the IDIM-IV approach described in section 2.2, with the instruments generated by the auxiliary model and the observation matrix again built using the conventional approach to differentiation; the third also uses an IDIM-IV approach, but with the observation matrix built with the `irwsm` function from the CAPTAIN Toolbox: this method is referred to as IDIM-IV(IRWSM1) because it is based on the $IRWSM_1$ variant discussed in section 3.4. The last method is a variant of the previous one where the GRW model contains three states, as defined in the $IRWSM_2$ variant in section 3.4, and this is referred to as IDIM-IV(IRWSM2). Both of these variants are provided as options in the `irwsmopt` and `irwsm` routines of the CAPTAIN Toolbox.

4.2. Robot identification with good a priori knowledge

Table 2 summarizes the identification results obtained from the analysis of the experimental data. The estimated values can be considered as satisfactory since they are similar to those found in previous studies on this robot: see e.g. [14]. Furthermore, the estimates lie in the 3σ interval around the IDIM-LS values. The IDIM-LS method can be seen as the reference methodology because the system's bandwidths are well-known. Figure 3 illustrates the experimental data and the identified model with this reference method. These satisfactory results are confirmed by low relative errors provided in Table 3.

Param.	IDIM-LS (Conventional)	IDIM-IV (Conventional)	IDIM-IV (IRWSM1)	IDIM-IV (IRWSM2)
zz_{1_r}	1.24 (1.20 %)	1.25 (1.27 %)	1.25 (1.28 %)	1.25 (1.29 %)
fc_1	7.29 (1.99 %)	7.26 (2.11 %)	7.22 (2.13 %)	7.21 (2.15 %)
fv_1	7.95 (0.66 %)	7.94 (0.68 %)	7.96 (0.68 %)	7.95 (0.96 %)
xx_{2_r}	-0.47 (2.68 %)	-0.47 (2.95 %)	-0.47 (3.00 %)	-0.46 (3.08 %)
xz_{2_r}	-0.16 (4.10 %)	-0.16 (5.02 %)	-0.16 (4.99 %)	-0.17 (4.86 %)
zz_{2_r}	1.09 (0.99 %)	1.09 (1.02 %)	1.09 (1.03 %)	1.10 (1.03 %)
mx_{2_r}	2.21 (2.17 %)	2.25 (2.80 %)	2.26 (2.81 %)	2.27 (2.82 %)
fc_2	8.24 (1.60 %)	8.34 (1.62 %)	8.32 (1.63 %)	8.32 (1.65 %)
fv_2	5.51 (1.05 %)	5.45 (1.08 %)	5.47 (1.09 %)	5.47 (1.10 %)
xx_{3_r}	0.14 (8.50 %)	0.13 (9.15 %)	0.13 (9.12 %)	0.13 (9.23 %)
zz_{3_r}	0.11 (8.30 %)	0.12 (8.59 %)	0.12 (8.57 %)	0.12 (8.56 %)
my_{3_r}	-0.60 (2.32 %)	-0.59 (2.37 %)	-0.59 (2.39 %)	-0.59 (2.42 %)
ia_3	0.09 (8.47 %)	0.09 (9.31 %)	0.09 (9.33 %)	0.09 (9.50 %)
fc_3	6.47 (2.03 %)	6.54 (2.08 %)	6.55 (2.09 %)	6.55 (2.11 %)
fv_3	1.93 (2.02 %)	1.92 (2.07 %)	1.92 (2.08 %)	1.92 (2.10 %)
mx_4	-0.02 (29.5 %)	-0.03 (28.5 %)	-0.03 (28.2 %)	-0.03 (28.5 %)
ia_4	0.03 (14.8 %)	0.03 (14.1 %)	0.03 (14.3 %)	0.03 (14.4 %)
fc_4	2.55 (5.60 %)	2.51 (5.83 %)	2.50 (5.87 %)	2.50 (5.91 %)
fv_4	1.09 (3.59 %)	1.10 (3.63 %)	1.10 (3.64 %)	1.10 (3.67 %)
my_{5_r}	-0.03 (17.1 %)	-0.03 (16.7 %)	-0.04 (16.6 %)	-0.04 (16.0 %)
ia_5	0.04 (13.1 %)	0.04 (14.0 %)	0.04 (14.0 %)	0.04 (14.1 %)
fc_5	3.07 (4.31 %)	3.06 (4.40 %)	3.05 (4.43 %)	3.05 (4.47 %)
fv_5	1.80 (2.80 %)	1.80 (2.80 %)	1.80 (2.81 %)	1.80 (2.84 %)
ia_6	0.01 (27.2 %)	0.01 (32.1 %)	0.01 (33.9 %)	0.01 (35.9 %)
fc_6	0.27 (61.4 %)	0.26 (63.7 %)	0.26 (65.1 %)	0.25 (66.9 %)
fv_6	0.65 (3.76 %)	0.65 (3.96 %)	0.65 (3.97 %)	0.65 (4.00 %)
fc_{m6}	1.94 (5.88 %)	1.94 (5.96 %)	1.94 (5.98 %)	1.95 (6.00 %)
fv_{m6}	0.60 (3.22 %)	0.60 (3.29 %)	0.60 (3.30 %)	0.59 (3.34 %)

Tab. 2. Estimated parameters and relative standard deviations for the case with good a priori knowledge.

	IDIM-LS (Conventional)	IDIM-IV (Conventional)	IDIM-IV (IRWSM1)	IDIM-IV (IRWSM2)
Good knowledge	4.66 %	4.61 %	4.64 %	4.67 %
Poor knowledge	9.91 %	10.9 %	11.3 %	11.3 %
No knowledge	42.2 %*	–	37.3 %	82.2 %

* neither bandpass nor decimate filter in this case

Tab. 3. Direct comparison – Relative errors.

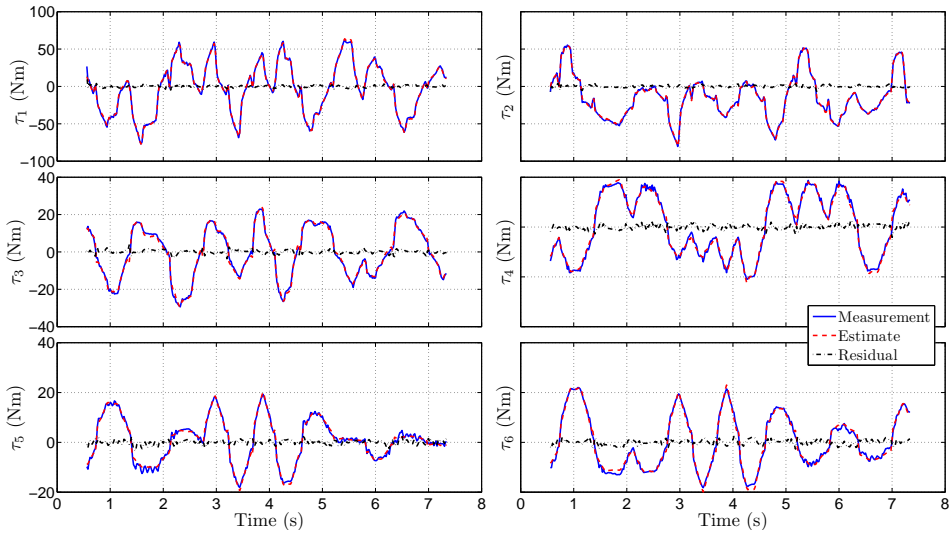


Fig. 3. IDIM-LS direct comparison: measurement (blue), estimate (dashed red) and residuals (dotted black) – Good a priori knowledge.

From these first identification results, it appears that, when the suggested simple IRWSM approach is used to estimate the joint velocities and accelerations, the identification results are comparable with those obtained using the conventional bandpass filter for differentiation. However, it is important to note that this first investigation has assumed good a priori knowledge in order to tune the bandpass and the decimation filters and this can be an issue in practice, especially if the system is totally unknown, as in the case of a robot bought off-the-shelf.

4.3. Robot identification with poor a priori knowledge

In order to challenge the robustness of the IRWSM approach to differentiation, we now consider the same experimental data but with incorrect knowledge about the system. In particular, the closed-loop bandwidth is assumed to be $\omega_{dyn} = 30$ Hz and, following the usual rules (see e. g. [10]), we take $\omega_q = 6\omega_{dyn}$, which leads to a 180 Hz cut-off frequency for the bandpass filter. With respect to the decimation filter, we use $\omega_f = 5\omega_{dyn} = 150$ Hz.

Table 4 summarizes the identification results with this poor a priori knowledge. First of all, the usual IDIM-LS method, with differentiation by the bandpass filtering, has difficulties which are especially visible with some inertia parameters highlighted in bold font, such as $zz_{3_r} = -0.02$. This illustrates the difficulty of the classical IDIM-LS method when the system bandwidth is not well-known and when non-optimal relations are used to set the filters. The relative errors provided in Table 3 do not highlight this difficulty because the observation matrices of the IV methods are significantly noisy. However, it is clear that the use of IV parameter estimation compensates for the presence of this noise.

Param.	IDIM-LS (Conventional)	IDIM-IV (Conventional)	IDIM-IV (IRWSM1)	IDIM-IV (IRWSM2)
zz_{1_r}	1.18 (0.65 %)	1.26 (0.78 %)	1.25 (0.48 %)	1.25 (0.57 %)
fc_1	7.12 (1.11 %)	7.19 (1.32 %)	7.14 (0.82 %)	7.13 (0.31 %)
fv_1	8.00 (0.36 %)	7.96 (0.42 %)	7.98 (0.26 %)	7.99 (0.31 %)
xx_{2_r}	-0.46 (1.44 %)	-0.47 (1.83 %)	-0.47 (1.12 %)	-0.47 (1.35 %)
xz_{2_r}	-0.16 (2.09 %)	-0.16 (3.12 %)	-0.16 (1.92 %)	-0.16 (2.29 %)
zz_{2_r}	0.99 (0.55 %)	1.09 (0.63 %)	1.10 (0.39 %)	1.09 (0.47 %)
mx_{2_r}	2.38 (1.10 %)	2.25 (1.74 %)	2.25 (1.08 %)	2.25 (1.29 %)
fc_2	8.36 (0.86 %)	8.29 (1.01 %)	8.26 (0.63 %)	8.26 (0.75 %)
fv_2	5.49 (0.58 %)	5.48 (0.67 %)	5.50 (0.41 %)	5.50 (0.49 %)
xx_{3_r}	0.14 (4.37 %)	0.13 (5.73 %)	0.13 (3.49 %)	0.13 (4.13 %)
zz_{3_r}	-0.02 (17.3 %)	0.12 (4.99 %)	0.12 (3.15 %)	0.12 (3.64 %)
my_{3_r}	-0.66 (1.07 %)	-0.59 (1.48 %)	-0.59 (0.91 %)	-0.58 (1.09 %)
ia_3	0.14 (2.67 %)	0.09 (5.96 %)	0.09 (3.64 %)	0.09 (4.34 %)
fc_3	6.24 (1.15 %)	6.52 (1.29 %)	6.50 (0.80 %)	6.52 (0.95 %)
fv_3	1.96 (1.09 %)	1.93 (1.28 %)	1.94 (0.79 %)	1.93 (0.94 %)
mx_4	-0.001 (127 %)	-0.03 (18.4 %)	-0.03 (11.0 %)	-0.03 (13.2 %)
ia_4	0.03 (6.81 %)	0.03 (8.75 %)	0.03 (5.33 %)	0.03 (6.53 %)
fc_4	2.43 (3.20 %)	2.50 (3.63 %)	2.48 (2.24 %)	2.50 (2.67 %)
fv_4	1.13 (1.90 %)	1.10 (2.25 %)	1.10 (1.38 %)	1.10 (1.66 %)
my_{5_r}	-0.06 (4.94 %)	-0.03 (11.0 %)	-0.04 (6.15 %)	-0.03 (7.97 %)
ia_5	0.04 (5.44 %)	0.04 (8.26 %)	0.04 (4.99 %)	0.04 (5.91 %)
fc_5	3.07 (2.35 %)	3.08 (2.71 %)	3.07 (1.67 %)	3.08 (2.00 %)
fv_5	1.78 (1.54 %)	1.80 (1.74 %)	1.80 (1.07 %)	1.79 (1.29 %)
ia_6	0.01 (10.2 %)	0.01 (18.1 %)	0.01 (11.0 %)	0.01 (14.2 %)
fc_6	0.26 (34.6 %)	0.28 (37.4 %)	0.28 (22.3 %)	0.27 (27.8 %)
fv_6	0.65 (2.08 %)	0.65 (2.46 %)	0.65 (1.51 %)	0.65 (1.82 %)
fc_{m6}	1.96 (3.18 %)	1.93 (3.68 %)	1.91 (2.28 %)	1.93 (2.71 %)
fv_{m6}	0.59 (1.78 %)	0.60 (2.03 %)	0.60 (1.25 %)	0.60 (1.50 %)

Tab. 4. Estimated parameters and relative standard deviations for the case with poor a priori knowledge.

	IDIM-IV (Conventional)	IDIM-IV (IRWSM1)	IDIM-IV (IRWSM2)
Good knowledge	3	3	3
Poor knowledge	7	4	3
No knowledge	–	4	3

Tab. 5. Number of iterations for the IDIM-IV methods.

Concerning the IDIM-IV methods, they provide similar results that are close to those obtained in section 4.2. The good robustness of the usual IDIM-IV method with respect to an incorrect setting of the filters is highlighted in [3]. The IRWSM approach for the

derivative estimation brings two advantages: firstly, the user does not have any concerns about the settings of the bandpass filters; and secondly, as shown in Table 5, the IRWSM requires less iterations to reach the convergence.

It should be noted that, although the relative standard deviations in Table 4 appear reasonable, they are not valid due to the wrong setting of the decimation filter, which results in the model residuals violating the theoretical requirement that they should be serially uncorrelated. This is confirmed by the autocorrelation results shown in Figure 4, where the autocorrelation estimates are well outside the confidence intervals (blue lines).

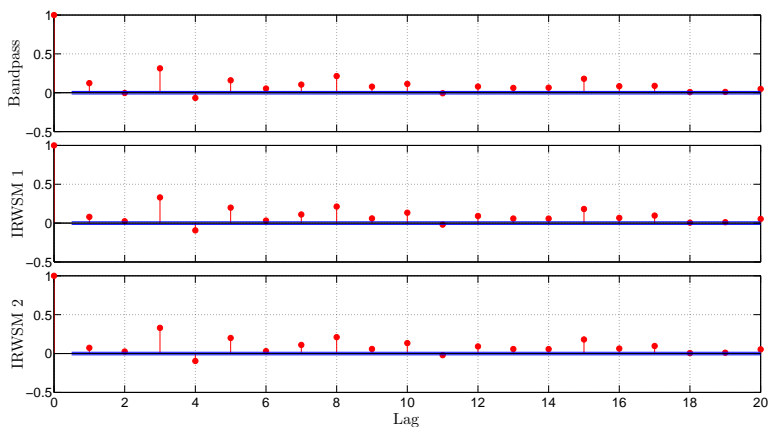


Fig. 4. Residuals autocorrelation – Poor a priori knowledge.

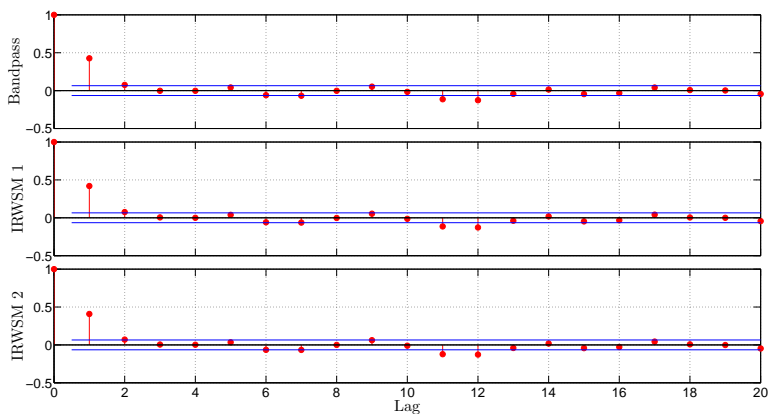


Fig. 5. Residuals autocorrelation – Good a priori knowledge.

For comparison, Figure 5 gives the autocorrelation of the residuals in the case of good a priori knowledge: these results are much better, although significant autocorrelation is detected at unity lag. Note that the difference in the confidence intervals between these two figures arises because the number of sampling points considered, N_s , is different because this depends on the decimation cut-off frequency.

4.4. Robot identification without a priori knowledge

The last experimental case to consider is when there is no knowledge about the system's bandwidth. In a rather stark manner, the user can undertake the identification without the bandpass and decimation filters and then, as we see in Table 5, the IDIM-IV method without filtering does not converge in the limit of 20 iterations. The IDIM-LS results are presented in Table 6 but many of them are not acceptable; there are even negative inertia, like $zz_{3,r} = -0.04$. Therefore, the inconsistent estimated parameters are not highlighted in bold font here. The main interest in this table, however, lies in the two sets of IDIM-IV results using IRWSM1 IRWSM2 differentiation, respectively. Here, the estimation results are very similar to the values found in the previous cases, although, once again, the relative standard deviations are not accurate due to the serial autocorrelation in the residuals. With regard to the choice between the IRWSM1 or IRWSM2 options, this example suggests that the IRWSM2 approach provides a noisier observation matrix, showing that the estimated derivatives contains more disturbances. Overall, therefore, it is clear that, even in this very challenging situation, the proposed IRWSM approach to differentiation, with the IRWSM1 option operative, is robust, effective and superior to the conventional approach based on user-tuned band-pass filtering.

5. CONCLUSION

This paper reconsiders the IDIM-IV instrumental variable technique for robot model identification. The previously proposed IDIM-IV method relies on a 'tailor-made' pre-filtering of the experimental data to recover velocity and acceleration signals from the measured joint position signals; a method that relies on the modeller's knowledge of the system's bandwidth prior to the identification. This can be a burden if the robot has been purchased off-the-shelf with little information of this type provided; or for a non-expert in robotics who would need to tune the prefilters by a trial-and-error procedure. This paper has proposed an alternative Integrated Random Walk Smoothing (IRWSM) approach, based on a simple integrated random walk model and a combination of the Kalman Filter and a Fixed Interval Smoothing (KF/FIS) algorithms, where the optimal Noise Variance Ratio (NVR) hyper-parameter is obtained by maximum likelihood based on prediction error minimization. On the basis of the results obtained when applying this and the previously proposed methods to experimental data from a typical industrial robot, it can be concluded that the IDIM-IV method exploiting this IRWSM approach to pre-filtering has significant advantages over both the previously proposed method and the conventional IDIM-LS approach. In particular, it does not rely on prior knowledge about the robot bandwidth characteristics and appears to be more robust in the presence of noise. Therefore, if the practitioner has a doubt about the system's bandwidth, it should employ the IDIM-IV method based on the IRWSM approach.

Param.	IDIM-LS (No filter)	IDIM-IV (IRWSM1)	IDIM-IV (IRWSM2)
zz_{1_r}	0.07 (4.46 %)	1.25 (0.76 %)	1.25 (2.73 %)
fc_1	6.47 (1.39 %)	7.14 (1.31 %)	7.14 (4.72 %)
fv_1	8.14 (0.40 %)	7.99 (0.41 %)	7.98 (1.49 %)
xx_{2_r}	-0.07 (4.33 %)	-0.47 (1.79 %)	-0.47 (6.45 %)
xz_{2_r}	-0.02 (6.74 %)	-0.16 (3.06 %)	-0.16 (11.1 %)
zz_{2_r}	0.05 (3.12 %)	1.09 (0.62 %)	1.09 (2.23 %)
mx_{2_r}	4.02 (0.68 %)	2.25 (1.73 %)	2.25 (6.23 %)
fc_2	9.88 (0.83 %)	8.26 (1.00 %)	8.27 (3.62 %)
fv_2	4.34 (0.80 %)	5.50 (0.66 %)	5.50 (2.38 %)
xx_{3_r}	-0.03 (9.43 %)	0.13 (5.47 %)	0.13 (20.0 %)
zz_{3_r}	-0.04 (3.83 %)	0.12 (4.68 %)	0.12 (17.2 %)
my_{3_r}	-0.20 (1.96 %)	-0.59 (1.44 %)	-0.59 (5.16 %)
ia_3	0.06 (2.53 %)	0.09 (5.73 %)	0.09 (20.5 %)
fc_3	6.20 (1.33 %)	6.53 (1.28 %)	6.52 (4.62 %)
fv_3	2.10 (1.17 %)	1.93 (1.27 %)	1.93 (4.56 %)
mx_4	0.05 (2.98 %)	-0.03 (17.1 %)	-0.03 (60.6 %)
ia_4	0.01 (10.2 %)	0.03 (8.34 %)	0.03 (29.3 %)
fc_4	2.60 (3.45 %)	2.50 (3.59 %)	2.50 (12.9 %)
fv_4	1.13 (2.18 %)	1.10 (2.22 %)	1.10 (8.01 %)
my_{5_r}	-0.02 (8.15 %)	-0.03 (10.2 %)	-0.03 (36.4 %)
ia_5	0.01 (7.19 %)	0.04 (6.45 %)	0.04 (24.9 %)
fc_5	3.09 (2.70 %)	3.08 (2.66 %)	3.08 (9.58 %)
fv_5	1.77 (1.77 %)	1.79 (1.72 %)	1.80 (6.19 %)
ia_6	0.001 (21.3 %)	0.01 (14.5 %)	0.01 (56.8 %)
fc_6	0.25 (41.9 %)	0.27 (36.5 %)	0.28 (132 %)
fv_6	0.66 (2.38 %)	0.65 (2.42 %)	0.65 (8.71 %)
fc_{m6}	1.89 (3.81 %)	1.93 (3.60 %)	1.93 (13.0 %)
fv_{m6}	0.61 (1.99 %)	0.60 (2.00 %)	0.60 (7.21 %)

Tab. 6. Estimated parameters and relative standard deviations for the case without a priori knowledge.

Research is continuing on the introduction of additional prefilters to eliminate completely the autocorrelation in the model residuals and so provide more confidence in the estimated relative standard deviations; as well as developing new approaches to tuning of the decimation filters in an effort to further reduce reliance on prior knowledge of the robot characteristics. Furthermore, the combination of the IDIM-IV method and the IRWSM approach could be compared with other identification methods.

REFERENCES

- [1] P.R. Bélanger, P. Dobrovolny, A. Helmy, and X. Zhang: Estimation of angular velocity and acceleration from shaft-encoder measurements. *Int. J. Robotics Research* 17 (1998), 1225–1233. DOI:10.1177/027836499801701107
- [2] M. Brunot, A. Janot, and F. Carrillo: State Space Estimation Method for the Identification of an Industrial Robot Arm. In: *Proc. IFAC World Congress 50 (2017)* 1, pp. 9815–9820.
- [3] M. Brunot, A. Janot, F. Carrillo, H. Garnier, P.-O. Vandanjon, and M. Gautier: Physical parameter identification of a one-degree-of-freedom electromechanical system operating in closed loop. In: *Proc. 17th IFAC Symposium on System Identification, 2015*, pp. 823–828. DOI:10.1016/j.ifacol.2015.12.231
- [4] D. Coca and S.A. Billings: A direct approach to identification of nonlinear differential models from discrete data. *Mech. Systems Signal Process.* 13(5), (1999), 739–755. DOI:10.1006/mssp.1999.1230
- [5] M. Dridi, G. Scorletti, M. Smaoui, and D. Tournier: From theoretical differentiation methods to low-cost digital implementation. In: *IEEE International Symposium on Industrial Electronics 2010*, pp. 184–189. DOI:10.1109/isie.2010.5637595
- [6] J. Durbin and S.J. Koopman: *Time Series Analysis by State Space Methods*. Oxford University Press, 2012. DOI:10.1093/acprof:oso/9780199641178.001.0001
- [7] H. Garnier, M. Gilson, P.C. Young, and E. Huselstein: An optimal IV technique for identifying continuous-time transfer function model of multiple input systems. *Control Engrg. Practice* 15 (2007), 471–486. DOI:10.1016/j.conengprac.2006.09.004
- [8] H. Garnier, M. Mensler, and A. Richard: Continuous-time model identification from sampled data: implementation issues and performance evaluation. *Int. J. Control*, 76 (2003), 1337–1357. DOI:10.1080/0020717031000149636
- [9] M. Gautier: Dynamic identification of robots with power model. In: *Proc. IEEE International Conference on Robotics and Automation 3 (1997)*, 1922–1927. DOI:10.1109/robot.1997.619069
- [10] M. Gautier, A. Janot, and P.-O. Vandanjon: A new closed-loop output error method for parameter identification of robot dynamics. *IEEE Trans. Control Systems Technol.* 21 (2013), 428–444. DOI:10.1109/tcst.2012.2185697
- [11] M. Gautier and W. Khalil: Exciting trajectories for the identification of base inertial parameters of robots. *Int. J. Robotics Research* 11 (1992), 362–375. DOI:10.1177/027836499201100408
- [12] M. Gilson, H. Garnier, P.C. Young, and P.M.J. Van den Hof: An instrumental variable approach for rigid industrial robots identification. *IET Control Theory Appl.* 5 (2011), 1147–1154. DOI:10.1049/iet-cta.2009.0476
- [13] A. Janot, P.-O. Vandanjon, and M. Gautier: An instrumental variable approach for rigid industrial robots identification. *Control Engrg. Practice* 25 (2014), 85–101. DOI:10.1016/j.conengprac.2013.12.009
- [14] A. Janot, P.-O. Vandanjon, and M. Gautier: A generic instrumental variable approach for industrial robot identification. *IEEE Trans. Control Systems Technol.* 22 (2014), 132–145. DOI:10.1109/tcst.2013.2246163
- [15] W. Khalil and E. Dombre: *Modeling, Identification and Control of Robots*. Butterworth-Heinemann, 2004.

- [16] K. Mahata and H. Garnier: Identification of continuous-time errors-in-variables models. *Automatica* 42 (2006), 1477–1490. DOI:10.1016/j.automatica.2006.04.012
- [17] N. Marcassus, P.-O. Vandanjon, A. Janot, and M. Gautier: Minimal resolution needed for an accurate parametric identification-application to an industrial robot arm. In: Proc. IEEE/RSJ International Conference on Intelligent Robots and Systems 2007, pp. 2455–2460. DOI:10.1109/iro.2007.4399476
- [18] J.P. Norton: Optimal smoothing in the identification of linear time-varying systems. In: Proc. of the Institution of Electrical Engineers 122 (1975), pp. 663–668. DOI:10.1049/piee.1975.0183
- [19] G.P. Rao and H. Unbehauen: Identification of continuous-time systems. *IEE Proc. Control Theory Appl.* 153 (2006), 185–220. DOI:10.1049/ip-cta:20045250
- [20] T. Söderström and P. Stoica: Instrumental Variable Methods for System Identification. Springer, 1983. DOI:10.1049/ip-cta:20045250
- [21] Stäubli Favergues: Arm – TX Series 40 Family. Stäubli, 2015.
- [22] J. M. Wooldridge: Introductory Econometrics: A Modern Approach. Fourth edition. South-Western, 2008.
- [23] P. C. Young: An instrumental variable method for real-time identification of a noisy process *Automatica*, 6 (1970), 271–287. DOI:10.1016/0005-1098(70)90098-1
- [24] P. C. Young: Recursive Estimation and Time-Series Analysis: An Introduction for The Student and Practitioner. Second edition. Springer Science and Business Media, 2012.
- [25] P. C. Young: Refined instrumental variable estimation: Maximum likelihood optimization of a unified Box-Jenkins model. *Automatica* 52, (2015), 35–46. DOI:10.1016/j.automatica.2014.10.126
- [26] P. C. Young, M. Foster, and M. Lees: A Direct Approach to the Identification and Estimation of Continuous-Time Systems From Discrete-Time Data Based on Fixed Interval Smoothing. In: Proc. 12th IFAC World Congress 10 (1993), pp. 27–30. DOI:10.1016/s1474-6670(17)49207-x
- [27] P. C. Young and A. J. Jakeman: Refined instrumental variable methods of time-series analysis: Parts I, II and III *Int. J. Control* 29, 1-30; 30, 621–644, 31, (1979–1980), 741–764. DOI:10.1080/00207178008961080

Mathieu Brunot, ONERA, 2 Avenue Edouard Belin, 31055 Toulouse, France; LGP ENI Tarbes, 47 avenue d’Azereix, BP 1629, 65016 Tarbes. France.
e-mail: Mathieu.Brunot@onera.fr

Alexandre Janot, ONERA, 2 Avenue Edouard Belin, 31055 Toulouse. France.
e-mail: Alexandre.Janot@onera.fr

Peter Young, Systems and Control Group, Lancaster Environment Centre, Lancaster University, United Kingdom and Integrated Catchment Assessment and Management Centre, Australian National University College of Medicine, Biology & Environment, Canberra, ACT.
e-mail: p.young@lancaster.ac.uk

Francisco Carrillo, LGP ENI Tarbes, 47 avenue d’Azereix, BP 1629, 65016 Tarbes. France.
e-mail: Francisco.Carrillo@enit.fr